THE JOURNAL OF PHYSICAL CHEMISTRY C

Article

pubs.acs.org/JPCC

Formation of Magic Isophorone Islands on Au(111): Interplay between Dipole Interactions and Hydrogen Bonding

Yi Cui,[†,⊥] Yi Pan,[‡,⊥] Thomas Meyer,[§] and Niklas Nilius*[,§]

[†]Vacuum Interconnected Nanotech Workstation, Suzhou Institute of Nano-Tech and Nano-Bionics, Chinese Academy of Sciences, Suzhou 215123, China

[‡]State Key Laboratory for Mechanical Behavior of Materials, Xi'an Jiaotong University, Xi'an 710049, China

[§]Institute of Physics, Carl von Ossietzky University, 26111 Oldenburg, Germany

ABSTRACT: Isophorone ($C_9H_{14}O$) adsorption is studied on the Au(111) surface by means of low-temperature scanning tunneling microscopy. Formation of magic islands, containing four, six, and nine molecules in distinct geometries, is revealed at intermediate coverage. The island formation is traced back to the interplay of dipole−dipole interactions, hydrogen bonding, and repulsive contributions between the side groups of adjacent molecules. The observed island geometries suggest chiral ordering of isophorone on the Au(111) surface.

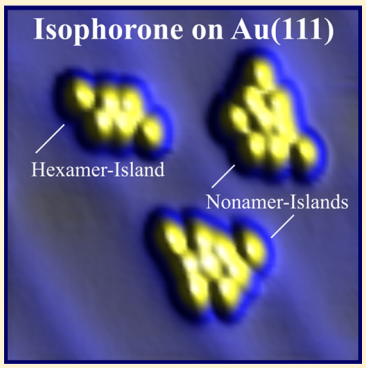

INTRODUCTION

The self-assembly of organic molecules on crystalline surfaces, in particular on Au(111), Ag(111) and HOPG(0001), has been extensively studied with scanning probe techniques in the past.[1,2] The fundamental interest in such experiments arises from the academic quest to gain better understanding of intermolecular interactions and their role in the observed ordering processes. From a more applied point of view, structure formation in molecular ensembles is considered to be a first step to develop functional devices, e.g., organic-thin films for molecular electronics, luminescence, and photovoltaics.[3] Self-assembly processes occur spontaneously on flat surfaces due to the impact of intermolecular forces, or can be triggered by template effects of suitable supports.[4] Recently, on-surface reactions have been exploited to visualize pattern formation *in situ*.[5,6]

The complexity of 2D ordering phenomena on surfaces reflects the diversity of intermolecular interaction schemes.[2,7] The strongest coupling is typically induced by covalent bonds that either form between molecular side groups, e.g., thio- or amino-groups, or through metal adatoms located in between two molecules.[8,9] Given the directional character of covalent bonds, the resulting networks often exhibit a distinct 2-, 3- or 4-fold symmetry.[10−12] Electrostatic interactions, on the other hand, are more long-ranged and thus weaker. They originate from charged functional groups or uneven electron distributions inside the molecules.[13,14] Charge-driven ordering effects have been revealed for oppositely charged molecules that typically agglomerate in the form of donor−acceptor pairs.[15,16] Also, dipole forces between molecular species have been linked to pattern formation, as shown for carboranethiols on Au(111).[17] Closely related to charge-mediated coupling is hydrogen bonding, in which the electropositive hydrogen of one molecule is attracted to the negative ion (O, Cl, F) of another.[1,18] Hydrogen bonding gives rise to a universal interaction length of 2−2.5 Å, and governs, for example, the pairing of DNA strings and the cohesion of H_2O molecules. Fluctuating charges and the concomitant polarization effects produce attractive van der Waals forces between molecules. Given their notorious weakness, they become important only if other coupling schemes are absent. In any case, the attractive intermolecular forces are balanced by repulsive interactions that govern the distance between neighboring entities and hence the nature of the molecular network.[1,2,14]

In most studies, molecular self-assembly has been addressed in the limit of extended films and large islands. Experiments on molecular clusters, comprising only a few constituents, are rarely found in the literature, although they provide even better insights into relevant coupling schemes.[19,20] Of particular interest in this respect are so-called "magic" clusters, being characterized by unique geometries and high thermodynamic stability. As magic clusters occur more frequently than their "nonmagic" counterparts, they play a crucial role as building blocks in extended molecular networks and hierarchical assemblies.[21,22]

In this study we discuss the adsorption characteristic of isophorone on Au(111), as probed with a scanning tunneling microscope (STM). Isophorone, an unsaturated cyclic ketone,

Received: November 23, 2016
Revised: January 24, 2017
Published: January 25, 2017

DOI: 10.1021/acs.jpcc.6b11781
J. Phys. Chem. C 2017, 121, 4318−4323

aggregates to nanoislands containing three to 12 molecules, whereby six- and nine-membered structures are particularly abundant. We assign the observed ordering effects to dipole−dipole coupling combined with hydrogen bonding, the latter being induced by the negatively charged O-ions in the molecules. The peculiar geometries of the observed nanoislands are compatible with the concept of chiral ordering. Our work thus unravels the surprisingly complex interaction behavior of a relatively simple organic molecule.

EXPERIMENT

The experiments have been performed with an ultrahigh-vacuum STM operated at 5 K. The Au(111) surface was prepared by alternating cycles of Ar^+ sputtering and heating to 800 K, producing the gold herringbone reconstruction on the entire surface. Liquid isophorone was purified by several freeze−pump−thaw cycles prior to the experiments. Because of its high vapor pressure, the molecules could directly be dosed from a flask onto the freshly prepared surface at room temperature. The exposure time was varied between 10 and 100 s at 10^{-8} mbar partial pressure. The samples were transferred into the cryogenic STM immediately after exposure to avoid contamination by the rest gas.

The probe molecule, isophorone ($C_9H_{14}O$), is composed of an unsaturated C_6 ring, hosting one C═C double bond and three CH_3 side groups (Figure 1). Main functional unit is a

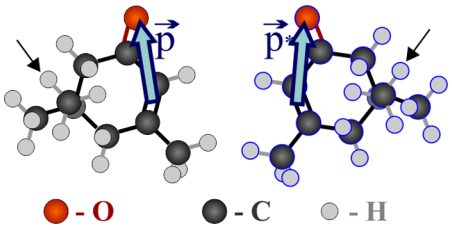

Figure 1. Ball models of the two isophorone enantiomers with their intrinsic dipole. The adsorbed molecule is of chiral nature due to the orientation of the CH_3 side groups marked by arrows that point out of the image plane in both cases.

double−bonded oxygen (carbonyl oxygen), located close to the C═C ring bond. The carbonyl oxygen serves as negative charge center of the molecule and produces, in combination with the electropositive C═C bond, a dipole of about 5 D. Surface-bound species are of chiral nature, as the CH_3 side-group opposite to the C═C ring bond points away from the surface in both enantiomers to reduce molecular tilting (Figure 1).[23,24] Isophorone has recently attracted attention, as it can be used to sense excess charges in metal-oxide systems used to mimic heterogeneous catalysts.[25]

RESULTS AND DISCUSSION

Coverage Dependent Adsorption Behavior. Individual isophorone molecules appear as round protrusions of ∼2.4 Å height and 12−14 Å diameter on the Au(111) surface (Figure 2a). No internal structure is resolved at bias voltages between −1.0 and +1.0 V, suggesting that the C_6 ring and not the carbonyl oxygen dominates the image contrast. Because of their circular appearance, the surface orientation of the molecules cannot be determined from the STM images. At low exposure, only individual molecules that typically bind to the ridges of the gold herringbone reconstruction are detected (Figure 2a). Not all molecules appear with identical contrast, which is ascribed to variations in their binding behavior to the structurally inhomogeneous Au(111) support. With increasing coverage, small islands develop at the herringbone elbows (Figure 2b). Although a variety of molecular structures is observed on the surface, certain sizes and shapes appear more frequent than others.

A compilation of such "magic" islands together with a histogram of their occurrence is depicted in Figure 3. Evidently, six-membered islands are most abundant and make up 40% of the total population, followed by four-and nine-membered structures both appearing with about 14% at small coverage. The magic islands are found in three orientations, reflecting the symmetry of the Au(111) support, but adopt very distinct and reproducible geometries otherwise. For example, the hexamer in the top panel of Figure 3b is composed of two triangles that directly face each other, while the distinctively different hexamer at the bottom comprises a central rhomboid, flanked by two distant molecules. The two nonamers in Figure 3c are nearly identical except their rotation angle that differs by 60°. The intermolecular distances measured in the isophorone islands fall into two groups, centered at 6.5 and 8.5 Å, respectively. This bimodality is clearly discernible for the hexamer in Figure 3b (bottom), being characterized by a dense packing in the center but larger distances to the outer molecules. The sequence of short and long intermolecular intervals is characteristic for a given island type and underlines their magic nature. It also explains, why isophorone does not undergo a simple hexagonal ordering on the Au(111) surface. We connect the occurrence of two specific molecular separations with the fact that more than one interaction scheme governs the aggregation of isophorone.

At higher exposure, the magic clusters disappear in favor of large ad-islands that contain several dozens of molecules. The

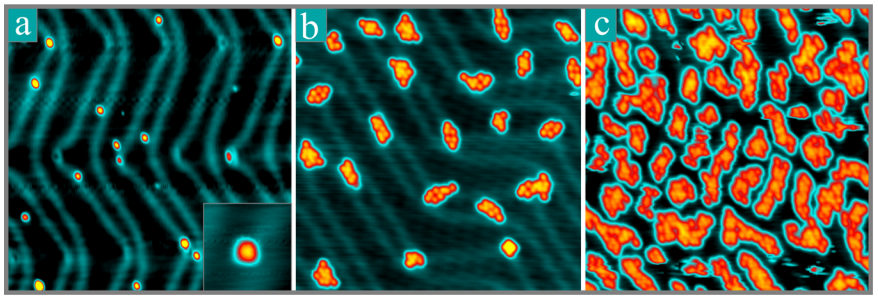

Figure 2. STM topographic images of Au(111) exposed to increasing amounts of isophorone at room temperature (−0.6 V, 0.1 nA, 43 × 43 nm^2). No internal structure can be resolved for the individual molecules, as reflected in the inset of panel a (4 × 4 nm^2).

DOI: 10.1021/acs.jpcc.6b11781
J. Phys. Chem. C 2017, 121, 4318−4323

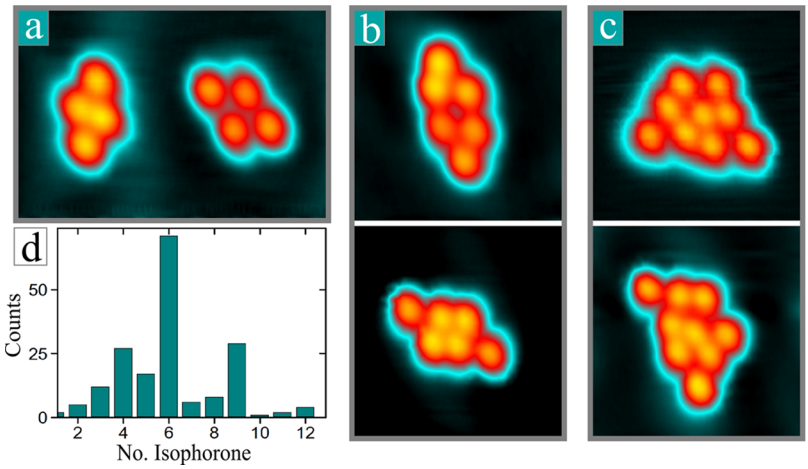

Figure 3. STM topographic images of magic (a) four- (−0.5 V, 0.1 nA, 5 × 7 nm^2), (b) six- and (c) nine-membered isophorone islands on Au(111) (5 × 5 nm^2). (d) Histogram of differently sized molecular islands, as revealed from a few dozens of STM images.

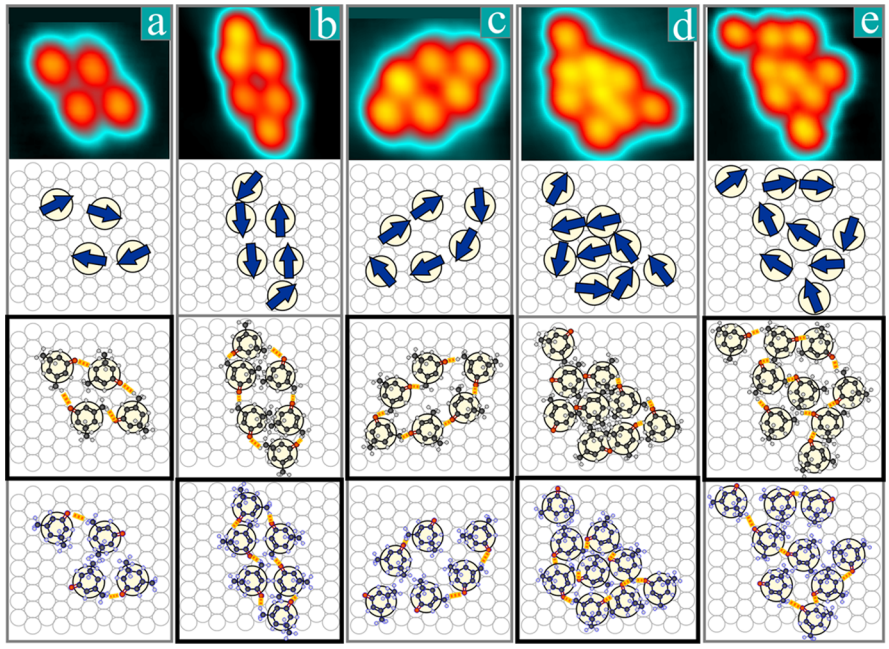

Figure 4. STM topographies, calculated low-energy dipole patterns and associated structure models for five magic isophorone islands on Au(111). The dipole orientations have been derived from optimizing dipole−dipole coupling in the experimentally observed clusters. When translating these dipole patterns into structure models, two molecular arrangements need to be considered for symmetry reasons. Those are depicted in the third and fourth row of the figure, which also shows possible hydrogen bonds as dashed, yellow lines. From the two possible configurations, one is typically in better agreement with the concepts of hydrogen bonding and shows reduced steric repulsion. This configuration is highlighted by a bold frame and might be thermodynamically preferred. See text for further details.

elongated aggregates largely follow the zigzag pattern of the gold herringbone reconstruction, whereby fcc- and hcp-regions directly adjacent to the ridges get covered first (Figure 2c). This binding preference mimics local reactivity variations, induced by the different stacking sequence of Au atoms in the herringbone reconstruction.[26] A complete isophorone layer can be produced only at very high exposure; while no second layer gets stabilized at room temperature. Let us stress that STM conductance spectra taken on isophorone did not unravel the molecular frontier orbitals. We rationalize this finding with the relatively wide HOMO−LUMO gap of this ketone that exceeds 4 eV according to DFT calculations.[27] In contrast, the energy window for conductance spectroscopy was limited to ±1.0 V, as the molecules started moving under the tip at higher voltage.

Intermolecular Interactions and Island Formation. The observation of magic isophorone islands indicates a subtle interplay of various intermolecular coupling schemes. While direct covalent bonding can be excluded due to the high degree of chemical saturation of the molecule, dipole−dipole attraction and hydrogen-bonding via the carbonyl oxygen may be responsible for molecular aggregation. Steric repulsion of the CH_3 sides groups, on the other hand, governs the distance between adjacent entities. Within the scope of this paper, we are unable to carry out full-scale *ab initio* calculations of the isophorone/Au(111) system, especially because relevant binding contributions, e.g., van der Waals forces, are weak and

DOI: 10.1021/acs.jpcc.6b11781
J. Phys. Chem. C 2017, 121, 4318−4323

require special treatment. To identify at least some general building principles of the magic clusters, we have concentrated on the role of electrostatic coupling and qualitatively checked the structural requirements for hydrogen bonding. As starting point, the relative coordinates of molecules inside the magic islands were determined from the STM images. We thereby assumed an on-top binding position of the C_6 ring on the Au(111) surface, as revealed from earlier work.[28] In accordance with the magic nature of the islands, the coordinates exhibit only a small spread for islands of the same type. By revolving the molecules around the derived positions, we maximized the dipole−dipole interactions for each molecular aggregate in a next step. Remember that isophorone exhibits a dipole moment $\vec{p}$ between its carbonyl oxygen and the C═C ring position. The total energy E_D arising from pairwise dipole coupling is given by:[29] $E_D = -\sum_{i>j} \frac{p_i p_j}{4\pi\varepsilon_0 r_{ij}^3}(\cos\Theta_{ij} - 3\cos\Theta_i \cos\Theta_j)$, with r_{ij} and Θ_{ij} being the distance and relative angle between two dipoles and Θ_i the tilting against the x-axis. To screen the full phase space, the dipole associated with each molecule was rotated by 360°, which implies sampling a nine-dimensional hyper-surface in the case of a nonamer cluster. Given the large number of possibilities, the angular resolution was set to 2° in the case of tetramer and hexamer clusters but reduced to 10° for nonamers.

The deduced dipole orientations are depicted in Figure 4 for five characteristic cluster types. Two alignment principles are discernible. In the tetramer and hexamer clusters, a row-wise dipole orientation prevails with a parallel alignment within a row and an antiparallel alignment between neighboring rows. For the more compact nonamers, a vortex-type dipole pattern is found in the quasi-hexagonal central unit, whereby the orientation of the inner dipole is rather unimportant for the total energy. The dipoles of the two molecules outside the vortex typically align parallel or antiparallel to their direct neighbors. We note that especially for nonamer clusters, a large number of nearly iso-energetic arrangements were found and, given the finite increments of rotation angles, the global energy minimum might have been missed. Nonetheless, the overall building principle with a central vortex-type arrangement and two correspondingly aligned outer dipoles is consistently found for all low-energy configurations. The impact of the polarizable Au support has been neglected in our calculations, as we are mainly interested in the role of intermolecular forces for pattern formation and not in absolute values of the interaction strength.

The two other relevant coupling schemes between isophorone molecules, hydrogen bonding and steric repulsion induced by the CH_3 side groups, cannot be assessed on this quantitative level. However, we may check whether the dipole configurations derived for the magic islands are compatible with the basic requirements for these interaction mechanisms. For this purpose, appropriately scaled ball models of isophorone were overlaid with the predicted dipole patterns, searching for conflicts in the molecular arrangements. For the tetramer island in its preferred dipole configuration, the molecules can be arranged without spatial overlap and hydrogen bonds are formed between all four carbonyl-oxygen and respective hydrogen atoms in adjacent molecules (Figure 4a, third row). Apparently, the proposed angular orientation of isophorone within the cluster is not in conflict with other mechanisms of molecular coupling. This situation changes for the hexamer cluster depicted in the Figure 4b. In the low-energy dipole configuration calculated for this structure, the CH_3 side groups of isophorone strongly overlap in the upper and lower triangular unit of the island, while a wide gap opens up in between. Moreover, oxygen−hydrogen distances between adjacent molecules are sometimes too large to enable hydrogen bonding. This molecular configuration thus appears unfavorable.

The specific symmetry of isophorone allows however for another molecular arrangement, as illustrated in the lower part of Figure 4b. In this case, the mirror images of isophorone have been arranged according to the calculated low-energy dipole pattern, which actually implies that the molecule is replaced by its chiral counterpart. The resulting structure seems favorable, as overlapping regions in the upper and lower parts of the island have disappeared and hydrogen bonding becomes possible in all six cases. Apparently, the new configuration fulfills the requirements for molecular interaction better than its counterpart. We have also explored mixed-chiral molecular assemblies that match both the geometric input from STM and the calculated dipole alignment. However, all tested arrangements have clear disadvantages with respect to the homochiral structure proposed in the fourth row of Figure 4b.

Similar results have been obtained for other magic islands studied in our work. The relatively open hexamer cluster in Figure 4c can be constructed with both enantiomers; however, the conditions for hydrogen bonding are clearly better in the upper arrangement, where six bonds can be established instead of three in the lower one. The preference for one chiral configuration becomes even clearer for the nine-membered aggregate shown in Figure 4d. The central region of this island appears highly crowed in the upper configuration, while most geometric conflicts are avoided in the lower one that seems also favorable for hydrogen bonding. Similar observations are made in the last example, the nonamer island shown in Figure 4e. While, several conflicts between molecular side groups occur in the lower configuration, the upper one looks somewhat more spacious. Moreover, the number of potential hydrogen bonds decreases from nine in the upper to six in the lower molecular assembly. In general, one chiral arrangement of the magic isophorone islands seems always preferred over the other one, at least on the basis of calculated dipole orientations and a by-eye judgment of hydrogen bonding. We note that these conclusions are mainly based on empirical arguments and cannot replace an *ab-inito* modeling of the system. Nonetheless, chiral ordering seems to be an option to explain the nature of magic isophorone islands on the Au(111) surface.

CONCLUSIONS

Low-temperature STM measurements revealed the formation of characteristic isophorone clusters on Au(111), such as six- and nine-membered aggregates. The distinct geometries of these islands have been explained with the interplay of three molecular coupling schemes that are dipole−dipole interactions, hydrogen bonding, and steric repulsion induced by the CH_3 side groups. In addition, the chiral nature of isophorone was considered, as the observed morphologies seem to be reproduced best if only one enantiomer is taken into account for island formation.

Chiral ordering has been connected to many self-assembly processes of organic molecules before and often gives rise to homochiral molecular domains.[30,31] Examples are the patterns of tartaric acid and adenine formed on Cu(110)[32,33] and the hierarchical structures of rubren on Ag(111) and Bi(111).[21,34] Unfortunately, we are unable to pinpoint the role of chirality

DOI: 10.1021/acs.jpcc.6b11781
J. Phys. Chem. C 2017, 121, 4318−4323

here, because the isophorone enantiomers could not be distinguished directly in the STM. Also other binding peculiarities of the molecule, e.g., its tendency to bind in a tilted fashion as found on Pd(111),[24] have not been considered in our interpretation. For more reliable adsorption scenarios, *ab initio* calculations are required that are however beyond the scope of this paper. The corresponding calculations are challenging due to the mere size of the molecular system and the notorious weakness of dipolar and van der Waals forces. Despite the empirical character of our approach, we have illuminated some relevant coupling schemes that might be behind the formation of magic isophorone islands on the Au(111) surface.

AUTHOR INFORMATION

Corresponding Author

*(N.N.) E-mail: niklas.nilius@uni-oldenburg.de. Telephone: +49-441-798-3152.

ORCID

Niklas Nilius: 0000-0003-0264-120X

Author Contributions

⊥Both authors contributed equally to this work

Notes

The authors declare no competing financial interest.

ACKNOWLEDGMENTS

We are grateful to H. Häkkinen and K. Honkala for their help in unraveling the properties of isophorone. TM thanks the Oldenburg Graduate School "Nanoenergy" for a fellowship. Y.C. is grateful to the NANO-X Workstation in Suzhou and the Chinese Thousand Young Talents Program. N.N. acknowledges financial support via a DFG grant, "Exploring photocatalytic processes at the nanoscale".

REFERENCES

(1) De Feyter, S.; De Schryver, F. C. Two-Dimensional Supramolecular Self-Assembly Probed by Scanning Tunneling Microscopy. *Chem. Soc. Rev.* **2003**, *32*, 139−150.

(2) Barth, J. V. Molecular Architectonic on Metal Surfaces. *Annu. Rev. Phys. Chem.* **2007**, *58*, 375−407.

(3) Tour, J. M. Molecular Electronics. Synthesis and Testing of Components. *Acc. Chem. Res.* **2000**, *33*, 791−804.

(4) Otsuki, J.; Nagamine, E.; Kondo, T.; Iwasaki, K.; Asakawa, M.; Miyake, K. J. Surface Patterning with Two-Dimensional Porphyrin Supramolecular Arrays. *J. Am. Chem. Soc.* **2005**, *127*, 10400−10405.

(5) Lackinger, M.; Heckl, W. M. A STM Perspective on Covalent Intermolecular Coupling Reactions on Surfaces. *J. Phys. D: Appl. Phys.* **2011**, *44*, 464011.

(6) Lafferentz, L.; Eberhardt, V.; Dri, C.; Africh, C.; Comelli, G.; Esch, F.; Hecht, S.; Grill, L. Controlling On-Surface Polymerization by Hierarchical and Substrate-Directed Growth. *Nat. Chem.* **2012**, *4*, 215−220.

(7) Reed, A. E.; Curtiss, L. A.; Weinhold, F. Intermolecular Interactions from a Natural Bond Orbital, Donor-Acceptor Viewpoint. *Chem. Rev.* **1988**, *88*, 899−926.

(8) Barth, J. V.; Costantini, G.; Kern, K. Engineering Atomic and Molecular Nanostructures at Surfaces. *Nature* **2005**, *437*, 671−679.

(9) Tahara, K.; Furukawa, S.; Uji-I, H.; Uchino, T.; Ichikawa, T.; Zhang, J.; Mamdouh, W.; Sonoda, M.; De Schryver, F. C.; De Feyter, S.; et al. Two-Dimensional Porous Molecular Networks of Dehydrobenzo-Annulene Derivatives Via Alkyl Chain Interdigitation. *J. Am. Chem. Soc.* **2006**, *128*, 16613−16625.

(10) Chung, K. H.; Park, J.; Kim, K. Y.; Yoon, J. K.; Kim, H.; Han, S.; Kahng, S. J. Polymorphic Porous Supramolecular Networks Mediated by Halogen Bonds On Ag(111). *Chem. Commun.* **2011**, *47*, 11492−11494.

(11) Li, Q.; Han, C.; Horton, S. R.; Fuentes-Cabrera, M.; Sumpter, B. G.; Lu, W.; Bernholc, J.; Maksymovych, P.; Pan, M. Supramolecular Self-Assembly of π-Conjugated Hydrocarbons via 2D Cooperative CH/π Interaction. *ACS Nano* **2012**, *6*, 566−572.

(12) Gong, Z.; Yang, B.; Lin, H.; Tang, Y.; Tang, Z.; Zhang, J.; Zhang, H.; Li, Y.; Xie, Y.; Li, Q.; Chi, L. Structural Variation in Surface-Supported Synthesis by Adjusting the Stoichiometric Ratio of the Reactants. *ACS Nano* **2016**, *10*, 4228−4235.

(13) Scudiero, L.; Hipps, K. W.; Barlow, D. E. A Self-Organized Two-Dimensional Bimolecular Structure. *J. Phys. Chem. B* **2003**, *107*, 2903−2909.

(14) Fernandez-Torrente, I.; Monturet, S.; Franke, K. J.; Fraxedas, J.; Lorente, N.; Pascual, J. I. Long-Range Repulsive Interaction Between Molecules on a Metal Surface Induced by Charge Transfer. *Phys. Rev. Lett.* **2007**, *99*, 176103.

(15) Umbach, T. R.; Fernandez-Torrente, I.; Ladenthin, J. N.; Pascual, J. I.; Franke, K. J. Enhanced Charge Transfer in a Monolayer of the Organic Charge Transfer Complex TTF-TNAP on Au(111). *J. Phys.: Condens. Matter* **2012**, *24*, 354003.

(16) Barlow, S. M.; Louafi, S.; Le Roux, D.; Williams, J.; Muryn, C.; Haq, S.; Raval, R. Supramolecular Assembly of Strongly Chemisorbed Size- and Shape-Defined Chiral Clusters: S- and R-Alanine on Cu(110). *Langmuir* **2004**, *20*, 7171−7176.

(17) Hohman, J. N.; Zhang, P. P.; Morin, E. I.; Han, P.; Kim, M.; Kurland, A. R.; McClanahan, P. D.; Balema, V. P.; Weiss, P. S. Self-Assembly of Carboranethiol Isomers on Au{111}: Intermolecular Interactions Determined by Molecular Dipole Orientations. *ACS Nano* **2009**, *3*, 527−536.

(18) Sherrington, D. C.; Taskinen, K. A. Self-Assembly in Synthetic Macromolecular Systems via Multiple Hydrogen Bonding Interactions. *Chem. Soc. Rev.* **2001**, *30*, 83−93.

(19) Böhringer, M.; Morgenstern, K.; Schneider, W. D.; Berndt, R. Two-Dimensional Self-Assembly of Magic Supramolecular Clusters. *J. Phys.: Condens. Matter* **1999**, *11*, 9871−9878.

(20) Katano, S.; Kim, Y.; Matsubara, H.; Kitagawa, T.; Kawai, M. Hierarchical Chiral Framework Based on a Rigid Adamantane Tripod on Au(111). *J. Am. Chem. Soc.* **2007**, *129*, 2511−2515.

(21) Pivetta, M.; Blum, M. C.; Patthey, F.; Schneider, W. D. Two-Dimensional Tiling by Rubrene Molecules Self-Assembled in Supramolecular Pentagons, Hexagons, and Heptagons on a Au(111) Surface. *Angew. Chem., Int. Ed.* **2008**, *47*, 1076−1079.

(22) Diller, K.; Klappenberger, F.; Allegretti, F.; Papageorgiou, A. C.; Fischer, S.; Wiengarten, A.; Joshi, S.; Seufert, K.; Ecija, D.; Auwärter, W.; et al. Investigating the Molecule-Substrate Interaction of Prototypic Tetrapyrrole Compounds: Adsorption and Self-Metalation of Porphine On Cu(111). *J. Chem. Phys.* **2013**, *138*, 154710.

(23) Mark, A. G.; Forster, M.; Raval, R. Recognition and Ordering at Surfaces: The Importance of Handedness and Footedness. *ChemPhysChem* **2011**, *12*, 1474−1480.

(24) Dostert, K. H.; O'Brien, C. P.; Riedel, W.; Savara, A. A.; Liu, W.; Oehzelt, M.; Tkatchenko, A.; Schauermann, S. Interaction of Isophorone with Pd(111): A Combination of IRAS, NEXAFS and DFT Studies. *J. Phys. Chem. C* **2014**, *118*, 27833−27842.

(25) Stiehler, C.; Calaza, F.; Schneider, W. D.; Nilius, N.; Freund, H. J. Molecular Adsorption Changes the Quantum Structure of Au Islands: Chemisorption Versus Physisorption. *Phys. Rev. Lett.* **2015**, *115*, 036804.

(26) Barth, J. V.; Brune, H.; Ertl, G.; Behm, R. J. STM Observations on the Reconstructed Au(111) Surface: Atomic Structure, Long-Range Superstructure, Rotational Domains, and Surface Defects. *Phys. Rev. B: Condens. Matter Mater. Phys.* **1990**, *42*, 9307.

(27) Stiehler, C.; Nilius, N.; Nevalaita, J.; Honkala, K.; Häkkinen, H. Gold/Isophorone Interaction Driven by Keto/Enol Tautomerization. *J. Phys. Chem. C* **2016**, *120*, 21962−21966.

(28) Yang, B.; Lin, X.; Pan, Y.; Nilius, N.; Freund, H. J.; Hulot, C.; Giraud, A.; Blechert, S.; Tosoni, S.; Sauer, J. Stabilizing Gold Adatoms

DOI: 10.1021/acs.jpcc.6b11781
J. Phys. Chem. C 2017, 121, 4318−4323

by Thiophenyl Derivates: A Possible Route Towards Metal Redispersion. *J. Am. Chem. Soc.* **2012**, *134*, 11161−11167.
(29) Kittel, C. *Introduction to Solid State Physics*; Wiley: New York, 2005.
(30) Ernst, K. H. Stereochemical Recognition of Helicenes on Metal Surfaces. *Acc. Chem. Res.* **2016**, *49*, 1182−1190.
(31) Mu, Z.; Shu, L.; Fuchs, H.; Mayor, M.; Chi, L. Two Dimensional Chiral Networks Emerging from the Aryl−F···H Hydrogen-Bond-Driven Self-Assembly of Partially Fluorinated Rigid Molecular Structures. *J. Am. Chem. Soc.* **2008**, *130*, 10840−10841.
(32) Lorenzo, M. O.; Haq, S.; Bertrams, T.; Murray, P.; Raval, R.; Baddeley, C. J. Creating Chiral Surfaces for Enantioselective Heterogeneous Catalysis: R,R-Tartaric Acid on Cu(110). *J. Phys. Chem. B* **1999**, *103*, 10661−10669.
(33) Chen, Q.; Frankel, D. J.; Richardson, N. V. Self-Assembly of Adenine on Cu(110) Surfaces. *Langmuir* **2002**, *18*, 3219−3225.
(34) Sun, K.; Lan, M.; Wang, J. Z. Absolute Configuration and Chiral Self-Assembly of Rubrene on Bi(111). *Phys. Chem. Chem. Phys.* **2015**, *17*, 26220−26224.

DOI: 10.1021/acs.jpcc.6b11781
J. Phys. Chem. C 2017, 121, 4318−4323